Supplementary information

Influence of redox-active components and particle size on reactive oxygen species production and oxidative potential of marine aerosols around the Arabian Peninsula

Haijie Tong,[1,2*] Steven Lelieveld,[2] Marco Wietzoreck,[2] Alexander Filippi,[2] Minas Iakovides,[3] Roman Prokeš,[4,5] Thomas Berkemeier,[2] Ulrich Pöschl,[2] Gerhard Lammel[2,4]

[1] Institute of Surface Science, Helmholtz-Zentrum Hereon, Geesthacht, Germany

[2] Multiphase Chemistry Department, Max Planck Institute for Chemistry, Mainz, Germany

[3] Climate and Atmosphere Research Centre, Cyprus Institute, Aglantzia, Cyprus

[4] RECETOX, Faculty of Science, Masaryk University, Brno, Czech Republic

[5] Global Change Research Institute. The Czech Academy of Sciences, Brno, Czech Republic

[*] *Correspondence to:* haijie.tong@hereon.de

Natural logarithmic size distribution of OP and redox-active components

Based on an assumption of the minimum size of collected particles to be 10 nm, we expressed the oxidative potential and chemical composition in terms of dlnDp in Figs. S2 and S3. Figure S2 shows that natural logarithmic size distributions of particle mass-normalized redox-active components, reactive oxygen species yields, and oxidative potential (OP) vary in the same order of $PM_{0.49\text{-}0.95}$>$PM_{3\text{-}7}$>$PM_{0.49}$. Figure S3 shows that natural logarithmic size distributions of sample air volume-normalized OP, H_2O_2 yields, EPFR concentrations, and WSTM concentrations vary in the same pattern as particle mass-normalized values (Fig. S2). The decreasing natural logarithmic OP from $PM_{0.49\text{-}0.95}$ to $PM_{3\text{-}7}$ and $PM_{0.49}$ around the Arabian Peninsula resembles the water-soluble OP of PM at a roadside site and an urban site in Atlanta, GA, USA.[1] Such a similarity confirms the significant exposure risk to accumulation-mode OP by PM with sizes ranging from 0.18 to 2.5 μm.

Sample air volume-based data

Compared to particle mass-normalized values (Fig. 2), the sample air volume-normalized results (see Fig. S4) show overall similar trends. However, the profiles of $Radicals_{aq}$ and WSTM exhibit differences, which is attributable to the variations of PM composition, PM redox-activity, and atmospheric PM concentrations ($PM_{2.5}$: 11-165 μg m^{-3}) among different days or places, also with regard to inorganic ions, dust and carbonaceous particles.[2] Figure S4 shows that sub-micrometer particles contribute more than coarse particles to averaged DTT_v (36-137 pmol min^{-1} m^{-3}), H_2O_2 (28-68

pmol m^{-3}), EPFR (0.003-7.8 × 10^{12} spins μg^{-1}), and $Radicals_{aq}$ (1.4-3.1 pmol m^{-3}). These mean values are overall lower than reported from urban continental sites, where the DTT_v, H_2O_2, and $Radicals_{aq}$ typically range from 100 to 4500 pmol min^{-1} m^{-3},[3-6] from 11 to 200 pmol m^{-3}, and from 3 to 7 pmol m^{-3},[7] respectively. DTT_v in these marine environments is also lower than most measurements reported from rural continental sites, which usually range from < 20 to 4000 pmol min^{-1} m^{-3}.[3, 5, 6, 8] In the few PM samples from the marine environments, namely the coastal and open Arabian Sea and Indian Ocean,[9-11] the DTT_v were higher than in the current study and ranged from 0.69 to 2.08 nmol DTT min^{-1} m^{-3}.

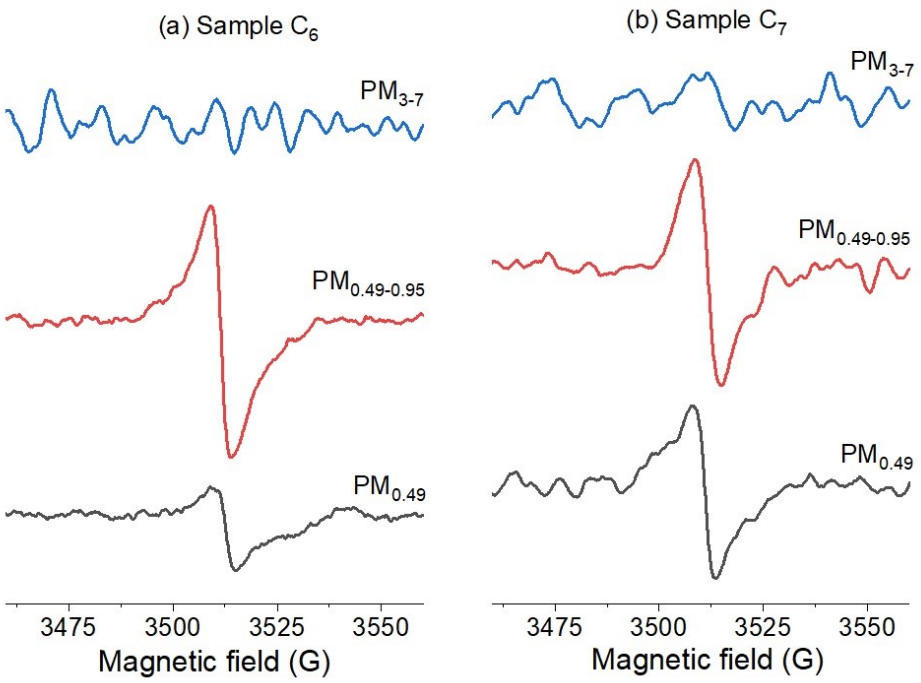

Fig. S1 EPR spectra of atmospheric aerosol impactor sample sets C6 (a) and C7 (b).

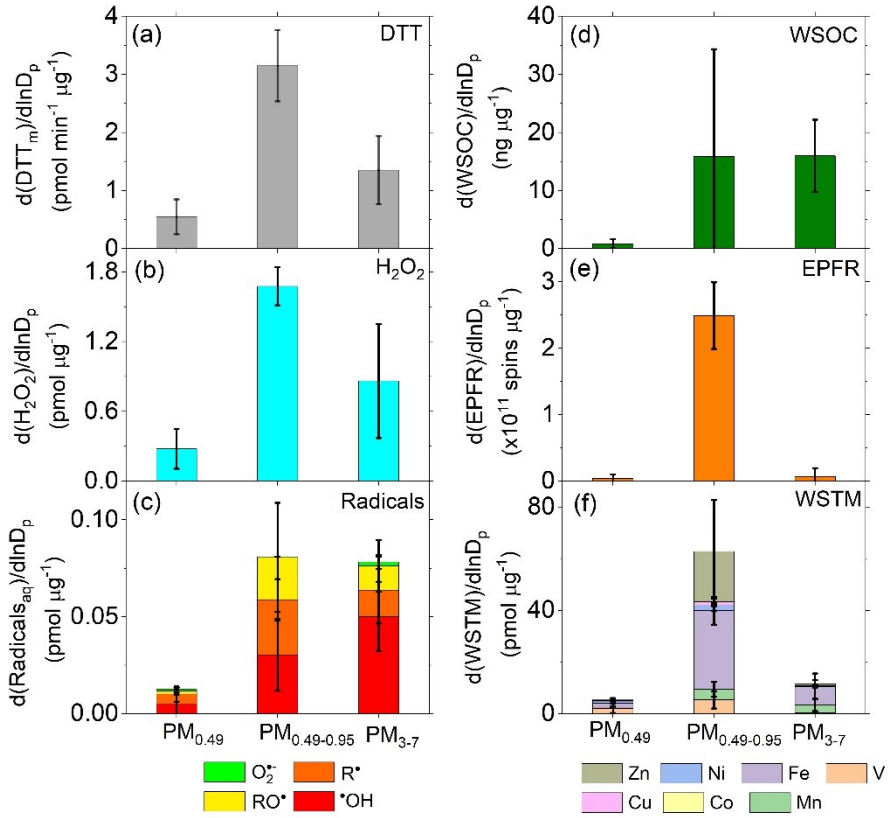

Fig. S2 Natural logarithmic size distributions of particle mass-normalized oxidative potential (OP), reactive oxygen species yields, and concentration of redox-active components.

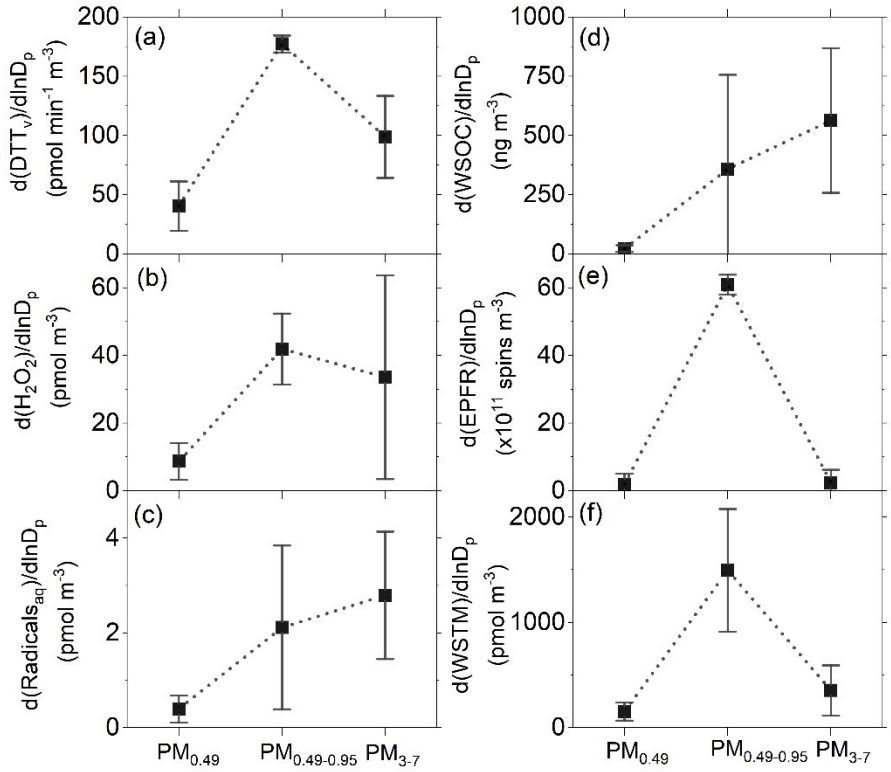

Fig. S3 Natural logarithmic size distributions of sample air volume-normalized oxidative potential (OP), reactive oxygen species yields, and concentration of redox-active components.

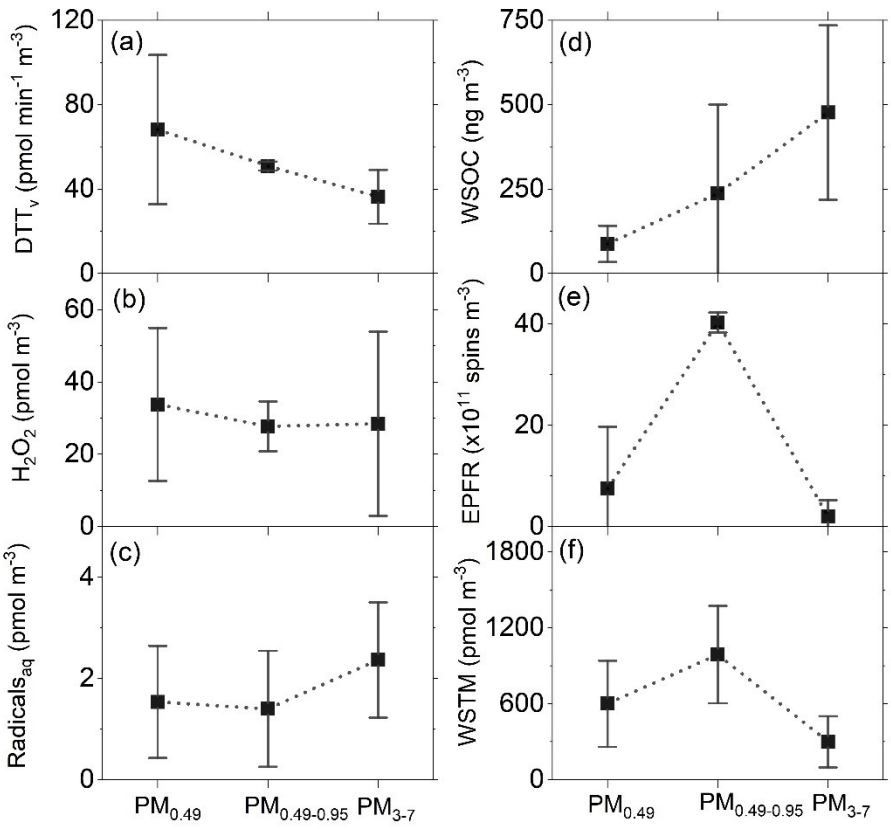

Fig. S4 Sample air volume-normalized mean values for oxidative potential (OP), reactive oxygen species yields, and concentration of target redox-active components of different size PM.

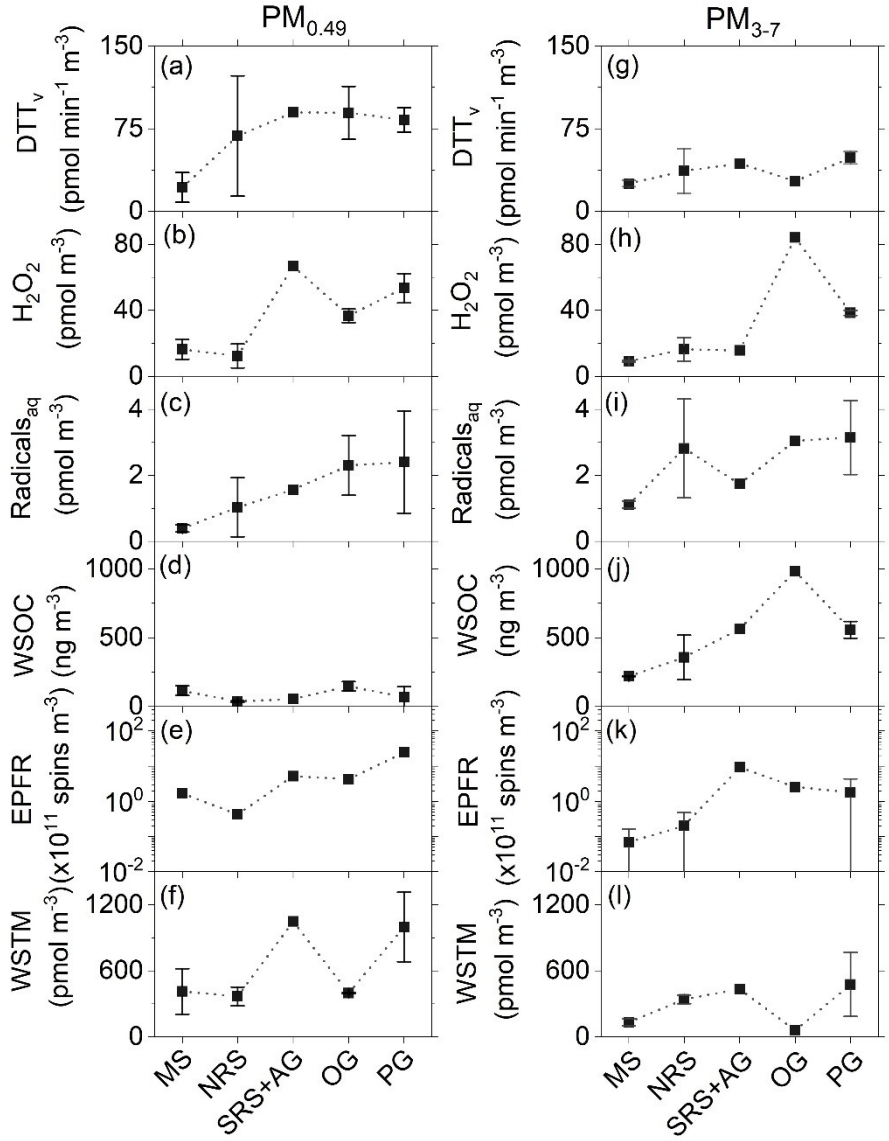

Fig. S5 Sample air volume-normalized mean values for oxidative potential (OP), reactive oxygen species yields, and concentrations of target redox-active components of $PM_{0.49}$ (a-f) and $PM_{3\text{-}7}$ (g-l) across different seas.

Table S1 Comparison of this study with literatures on OP of PM around the Arabian Peninsula.

Time	PM size	DTT_v	DTT_m	Analyzed components	Ref
		nmol min^{-1} m^{-3}	pmol min^{-1} μg^{-1}		
15/04/2017-03/05/2017	PM_{10}	0.69-2.08	6-26	EC, OC, WSOC, WSON, WSTM, WS ions	[9]
10/01/2014-03/02/2014 11/01/2017-21/04-2017	$PM_{2.5}$	1.3-10.1	13-58	EC, OC, WSOC, WSON, WSTN, WSTM, Acid-soluble metals	[11]
05/02/2013-17/04/2013 03/2014-05/2016 20/12/2015-16/02/2016 13/04/2017-03/05/2017 05/2017-06/2017	PM_{10}	0.1-6.4	2-93	EC, OC, WSOC, WSON, WSTN, WSTM, Acid-soluble metals, WS ions	
16/01/2018-14/02/2018	$PM_{2.5}$	0.08-3.23	6.74-43.48	EC, OC, WSOC, WSTM, WS ions	[10]
24/07/2017-27/08/2017	$PM_{0.49}$	0.012-0.107	0.4-3.6	WSOC, WSTM, EPFR, H_2O_2, Radicals	This study
	$PM_{0.49-0.95}$	0.049-0.052	1.8-2.4		
	PM_{3-7}	0.022-0.052	0.4-1.9		

Table S2 Oxidative potential (OP) of size-resolved PM at different marine sites and impactor collection-based atmospheric concentration of PM (particle mass in one cubic meter of sampled air).

Sample ID	Sampling site	Particle size	PM in impactor stage	DTT_m	H_2O_2	$Radicals_{aq}$			
						$^{\bullet}OH$	$R^{\bullet}$	$RO^{\bullet}$	$O_2^{\bullet-}$
			$\mu g\ m^{-3}$	$pmol\ min^{-1}\ \mu g^{-1}$	$pmol\ \mu g^{-1}$	$pmol\ \mu g^{-1}$			
C13B	AG+SRS	PM_{3-7}	31.3	1.39	0.50	0.030	0.0044	0.020	0.0014
C13F	AG+SRS	$PM_{0.49}$	36.0	2.49	1.85	0.028	0.0045	0.0041	0.0072
C19B	NRS	PM_{3-7}	26.5	1.92	0.81	0.057	0.0071	0.0012	0.0017
C19F	NRS	$PM_{0.49}$	29.9	3.58	0.24	0.017	0.0001	0.0008	0.020
C23B	NRS	PM_{3-7}	38.0	0.58	0.30	0.048	0.044	0.0001	0.0091
C23F	NRS	$PM_{0.49}$	13.5	2.21	1.29	0.0001	0.0001	0.0028	0.0001
C25B	MS	PM_{3-7}	20.7	1.11	0.46	0.041	0.0055	0.0039	0.0005
C25F	MS	$PM_{0.49}$	11.0	2.83	1.87	0.0001	0.0017	0.0004	0.0001
C26B	MS	PM_{3-7}	23.5	1.15	0.37	0.028	0.0016	0.021	0.0001
C26F	MS	$PM_{0.49}$	31.8	0.38	0.38	0.0001	0.0043	0.0002	0.0001
C27F	OG	$PM_{0.49}$	165.0	0.64	0.24	0.0001	0.001	0.0055	0.0001
C28F	OG	$PM_{0.49}$	19.9	3.64	1.70	0.060	0.032	0.011	0.0001
C3B	OG	PM_{3-7}	65.3	0.42	1.29	0.032	0.0085	0.0059	0.0001
C6B	PG	PM_{3-7}	52.3	1.00	0.71	0.071	0.0005	0.0035	0.27
C6E	PG	$PM_{0.49-0.95}$	27.5	1.80	1.19	0.029	0.024	0.028	0.0001
C6F	PG	$PM_{0.49}$	42.8	2.12	1.10	0.030	0.0071	0.023	0.0001
C7B	PG	PM_{3-7}	28.0	1.59	1.41	0.033	0.020	0.031	0.0007
C7E	PG	$PM_{0.49-0.95}$	22.1	2.37	1.03	0.011	0.014	0.0013	0.0001
C7F	PG	$PM_{0.49}$	55.1	1.36	1.08	0.0001	0.0077	0.0043	0.0001

Table S3 Abundance of redox-active components in PM samples.

Sample ID	EPFR	WSOC	V	Mn	Fe	Co	Ni	Cu	Zn
	spin μg^{-1}	ng μg^{-1}	pmol μg^{-1}						
C13B	2.97×10^{10}	18.11	0.33	2.77	10.51	0.017	0.18	0.095	0.040
C13F	1.43×10^{10}	0.77	7.91	0.93	14.55	0.040	3.68	0.69	1.36
C19B	4.55×10^{7}	17.75	0.23	2.21	8.98	0.018	0.071	0.12	0.22
C19F	1.74×10^{9}	0.54	5.97	0.14	1.53	0.014	2.11	0.50	0.071
C23B	1.04×10^{9}	6.39	0.15	3.92	5.54	0.019	0.022	0.032	0.002
C23F	2.50×10^{9}	1.47	17.03	0.91	6.94	0.045	5.44	0.37	0.96
C25B	6.53×10^{8}	10.60	0.24	1.89	4.65	0.014	0.066	0.088	0.67
C25F	2.40×10^{10}	4.08	22.24	0.67	10.33	0.064	10.25	0.85	6.47
C26B	1.00×10^{13}	9.30	0.27	1.55	2.48	0.009	0.10	0.073	0.17
C26F	2.26×10^{9}	2.18	3.62	0.19	2.28	0.013	1.26	0.19	0.83
C27F	4.46×10^{9}	0.37	0.36	0.11	0.85	0.003	0.59	0.14	0.38
C28F	6.42×10^{9}	4.28	4.93	1.08	6.73	0.024	4.23	1.28	1.51
C3B	3.90×10^{9}	15.05	0.16	0.44	0.24	0.001	0.047	0.031	0.002
C6B	4.81×10^{12}	9.84	0.15	1.22	3.68	0.005	0.038	0.098	0.008
C6E	1.42×10^{11}	1.85	0.002	0.001	0.018	0.001	0.001	0.001	0.004
C6F	2.46×10^{10}	0.20	4.70	0.83	7.61	0.019	2.021	1.88	1.07
C7B	1.30×10^{10}	21.40	0.55	6.87	12.52	0.058	0.33	0.45	3.58
C7E	1.89×10^{11}	19.15	0.005	0.004	0.023	0.001	0.001	0.002	0.022
C7F	7.04×10^{10}	1.11	5.20	0.80	9.25	0.027	2.26	1.40	3.24

s.

References

1. T. Fang, L. H. Zeng, D. Gao, V. Verma, A. B. Stefaniak and R. J. Weber, Ambient Size Distributions and Lung Deposition of Aerosol Dithiothreitol-Measured Oxidative Potential: Contrast between Soluble and Insoluble Particles, *Environ. Sci. Technol.*, 2017, **51**, 6802-6811, DOI: 10.1021/acs.est.7b01536.
2. D. G. Kaskaoutis, M. Pikridas, K. Barmpounis, G. Kassell, D. Logan, M. Rigler, M. Ivančič, K. Mohammadpour, N. Mihalopoulos, J. Lelieveld and J. Sciare, Aerosol characteristics and types in the marine environments surrounding the East Mediterranean - Middle East (EMME) region during the AQABA campaign, *Atmos. Environ.*, 2023, **298**, 119633, DOI: 10.1016/j.atmosenv.2023.119633.
3. K. R. Daellenbach, G. Uzu, J. H. Jiang, L. E. Cassagnes, Z. Leni, A. Vlachou, G. Stefenelli, F. Canonaco, S. Weber, A. Segers, J. J. P. Kuenen, M. Schaap, O. Favez, A. Albinet, S. Aksoyoglu, J. Dommen, U. Baltensperger, M. Geiser, I. el Haddad, J. L. Jaffrezo and A. S. H. Prévot, Sources of particulate-matter air pollution and its oxidative potential in Europe, *Nature*, 2020, **587**, 414-419, DOI: 10.1038/s41586-020-2902-8.
4. J. V. Puthussery, A. Singh, P. Rai, D. Bhattu, V. Kumar, P. Vats, M. Furger, N. Rastogi, J. G. Slowik, D. Ganguly, A. S. H. Prevot, S. N. Tripathi and V. Verma, Real-Time Measurements of $PM_{2.5}$ Oxidative Potential Using a Dithiothreitol Assay in Delhi, India, *Environ. Sci. Technol. Lett.*, 2020, **7**, 504-510, DOI: 10.1021/acs.estlett.0c00342.
5. H. R. Yu, J. V. Puthussery, Y. X. Wang and V. Verma, Spatiotemporal variability in the oxidative potential of ambient fine particulate matter in the Midwestern United States, *Atmos. Chem. Phys.*, 2021, **21**, 16363-16386, DOI: 10.5194/acp-21-16363-2021.
6. M. Vörösmarty, G. Uzu, J.-L. Jaffrezo, P. Dominutti, Z. Kertész, E. Papp and I. Salma, Oxidative potential in rural, suburban and city centre atmospheric environments in Central Europe, *Atmos. Chem. Phys.*, 2023, **23**, 14255–14269, DOI: 10.5194/acp-23-14255-2023.
7. H. J. Tong, F. B. Liu, A. Filippi, J. Wilson, A. M. Arangio, Y. Zhang, S. Y. Yue, S. Lelieveld, F. X. Shen, H. M. K. Keskinen, J. Li, H. X. Chen, T. Zhang, T. Hoffmann, P. Q. Fu, W. H. Brune, T. Petäjä, M. Kulmala, M. S. Yao, T. Berkemeier, M. Shiraiwa and U. Pöschl, Aqueous-phase reactive species formed by fine particulate matter from remote forests and polluted urban air, *Atmos. Chem. Phys.*, 2021, **21**, 10439-10455, DOI: 10.5194/acp-21-10439-2021.
8. L. J. Borlaza, S. Weber, A. Marsal, G. Uzu, V. Jacob, J. L. Besombes, M. Chatain, S. Conil and J. L. Jaffrezo, Nine-year trends of PM_{10} sources and oxidative potential in a rural background site in France, *Atmos. Chem. Phys.*, 2022, **22**, 8701-8723, DOI: 10.5194/acp-22-8701-2022.
9. A. Patel and N. Rastogi, Chemical Composition and Oxidative Potential of Atmospheric PM_{10} over the Arabian Sea, *ACS Earth Space Chem.*, 2020, **4**, 112-121, DOI: 10.1021/acsearthspacechem.9b00285.
10. S. Panda, S. S. Babu, S. K. Sharma, T. K. Mandal, T. Das and B. Ramasamy, Role of South Asian outflow on the oxidative potential of marine aerosols over the Indian Ocean, *Sci. Total Environ.*, 2023, **887**, 164105, DOI: 10.1016/j.scitotenv.2023.164105.
11. A. Patel and N. Rastogi, Oxidative Potential of Atmospheric Aerosols over Different Regions of India and Surrounding Oceans, *ACS Earth Space Chem.*, 2023, **7**, 2582-2592, DOI: 10.1021/acsearthspacechem.3c00250.